
Article:
Campo Rodrigo, Ana, Bromfield, Stephen, Laurini, Erik et al. (3 more authors) (2017) Morphological Control of Self-Assembled Multivalent (SAMul) Heparin Binding in Highly Competitive Media. Chemical Communications. pp. 6335-6338. ISSN: 1364-548X

https://doi.org/10.1039/c7cc02990j

Journal Name

COMMUNICATION

Morphological Control of Self-Assembled Multivalent (SAMul) Heparin Binding in Highly Competitive Media

Received 00th January 20xx,
Accepted 00th January 20xx

DOI: 10.1039/x0xx00000x

www.rsc.org/

Ana C. Rodrigo,[a] Stephen M. Bromfield,[a] Erik Laurini,[b] Paola Posocco,[b] Sabrina Pricl[b] and David K. Smith*[,a]

Tuning molecular structures of self-assembling multivalent (SAMul) dendritic cationic lipopeptides controls the self-assembled morphology. In buffer, spherical micelles formed by higher generation systems bind polyanionic heparin better than worm-like micelles formed by lower generation systems. In human serum, the binding of spherical micelles to heparin is adversely affected, while worm-like micelles maintain their relative binding ability.

Multivalency is crucial in achieving high-affinity binding in biological systems, amplifying weak binding events in highly competitive environments.[1] Self-assembly is a strategy by which 'bottom-up' fabrication of nanoscale systems can be achieved and has emerged as an effective way of organizing multiple ligands to enhance binding – 'self-assembled multivalency' (SAMul).[2] A range of SAMul systems for biomedical targets has been developed.[3] A few elegant studies have begun to focus on morphology,[4] but its impact on binding remains to be fully elucidated. Heparin, a polyanionic glycosaminoglycan is a target of considerable interest, due to its clinical applications.[5] There has been general interest in binding polyanions using colloidal polycations.[6] Self-assembled nanoscale systems such as liposomes have been used to bind heparin, primarily with the goal of enhancing liposome biocompatibility.[7] We have developed SAMul micelles with heparin binding potential, demonstrated they can have pharmaceutically-useful degradation profiles for heparin reversal,[8] and performed nanoscale structure-activity relationship studies – for example exploring the impact of ligand chirality on binding.[9] Self-assembled polymer micelles have also been bound to heparin to enhance drug delivery,[10] and Kostiainen and co-workers used cationic block copolymer micelles to bind heparin, modifying the cationic block to optimise binding.[11] A self-assembled approach to heparin binding has recently been explored by de Grado and co-workers who reported that self-assembly was enhanced in the presence of heparin and at high ionic strength.[12] Stupp and co-workers used heparin binding to nucleate the growth of cationic peptide nanofibres.[13] A key advantage of self-assembly is molecular-scale programmability by simple synthetic modification. In this paper, we report new dendritic lipopeptide SAMul ligands and report the impact of structural modification on self-assembled morphology, and hence polyanion binding.

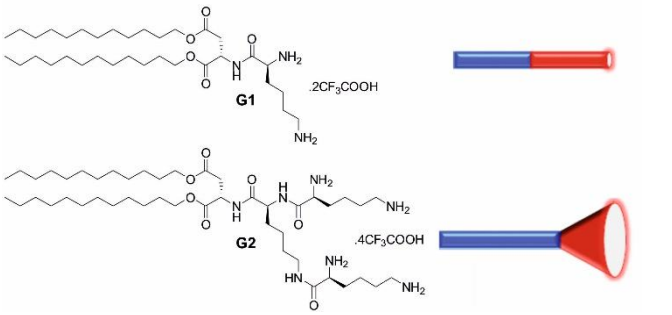

Figure 1. Structures of self-assembling dendrons **G1** and **G2** with a schematic of their molecular shapes.

We designed systems with different hydrophilic-lipophilic balances (HLBs)[14] using a dendritic hydrophilic ligand – amphiphilic dendrons are known to assemble well.[15] Dendritic cationic L-lysine ligands were synthesised and connected to twin aliphatic tails through ester bonds via an L-aspartic acid linker (Fig. 1). Synthesis of both L and D enantiomers was achieved using simple peptide chemistry and protecting group methodologies (see ESI). First generation **G1** was designed to be 'rod-like', while second generation **G2** has a more 'cone-like' structure. Multiscale modelling (see ESI for details) confirmed the molecular shapes and predicted **G1** would assemble into worm-like cylindrical micelles, while **G2** would form spherical micelles (Fig. 2). We initially anticipated worm-like micelles may be better shape-matched to heparin, and bind it more strongly.

We determined critical micelle concentrations (CMC^{NR}, Table 1) using a Nile Red assay.[16] Dendrons **G1** and **G2** had very different CMC values of 67 and 9 μM respectively, suggesting

[a] *Department of Chemistry, University of York, Heslington, York, YO10 5DD, UK. Email: david.smith@york.ac.uk*

Electronic Supplementary Information (ESI) available: synthesis and characterisation data, assay methods and additional data, TEM images, molecular modelling methodologies. See DOI: 10.1039/x0xx00000x

the 'cone-like' **G2** dendron is more effective in terms of self-assembly thermodynamics. Isothermal titration calorimetry (ITC) demicellization experiments confirmed the CMCs (CMC^{ITC}, Table 1). Further analysis of ITC data indicated that **G2** assembly is preferred on entropic grounds – with spherical micelles, a larger number of smaller nanoscale objects are formed (see ESI). Dynamic light scattering (DLS, Table 1) supported the view that **G1** formed larger assembled structures – in agreement with modelling. Given they are not spherical, the data cannot be fitted in a meaningful way, but indicated an equivalent average spherical diameter of ca. 125 nm. In contrast, **G2** gave well-defined assemblies with a diameter of 6.7 nm, consistent with the view from modelling that **G2** forms small spherical micelles. ζ-potential measurements indicated both systems formed cationic assemblies. Worm-like **G1** assemblies appeared more charge dense than **G2** spherical assemblies, suggesting a more densely packed, less open surface.

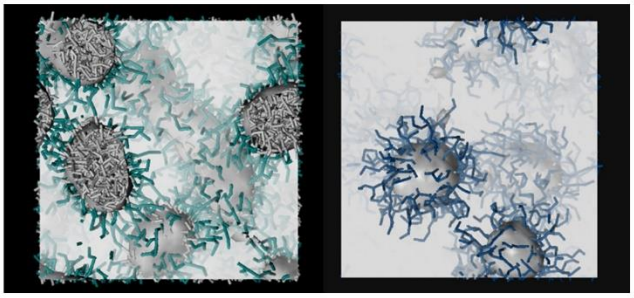

Figure 2. Worm-like (left) and spherical (right) micelles predicted from simulation of **G1** and **G2**, respectively, in solution. The hydrophobic core is highlighted as a grey-shaded surface (and grey sticks), while the hydrophilic shell is depicted as forest green and blue sticks for **G1** and **G2**, respectively.

Table 1. Critical Micelle Concentrations (CMCs) for G1 and G2 determined by Nile Red assay (PBS, 10 mM pH 7.4, 138 mM NaCl) and ITC experiments (Tris-HCl, 10 mM, pH 7.4, NaCl 150 mM) (CMC^{NR} and CMC^{ITC} respectively), and ζ–sizing data from DLS volume contribution (Tris-HCl, 10 mM, pH 7.4, NaCl 150 mM).

	G1	**G2**
CMC^{NR} / μM	67 ± 10	9 ± 1
CMC^{ITC} / μM	58	13
Diameter / nm	125 ± 10[a]	6.7 ± 0.2
ζ-Potential / mV	+73.2 ± 3.3[a]	+29.6 ± 2.3

a: The objects are non-spherical and data therefore only represent the sphere which would have the same average translational diffusion coefficient as the worm-like micelles.

We then determined the relative heparin binding affinities of **G1** and **G2** using our Mallard Blue (MalB) displacement assay.[17] This gives CE_{50} and EC_{50} values corresponding to the charge excess and concentration required to displace 50% of MalB dye from its complex with heparin.[17] It was evident (Table 2) that in buffer (10 mM Tris-HCl, 150 mM NaCl, pH 7.4), **G2-L**, which assembles into spherical micelles, was a much more effective heparin binder than **G1-L**, with worm-like micellar morphology. The same was observed for enantiomeric **G2-D** and **G1-D**. This was initially counter-intuitive, as we had anticipated that worm-like **G1** micelles may form more contacts with heparin – furthermore, they had higher apparent charge densities (Table 1) which should enhance binding.[6] We reasoned the higher CMC of **G1** may limit effective binding at lower concentrations, while the lower CMC of **G2** allows SAMul binding to be optimized. Indeed, the EC_{50} values are in good agreement with CMC values, suggesting self-assembly is a pre-requisite for effective heparin binding. Enantiomeric **G1-D** and **G2-D** were similar to **G1-L** and **G2-L** respectively, suggesting limited chiral discrimination at this nanoscale binding interface – in contrast to some of our previous studies.[9]

Table 2. Heparin Binding Parameters for G1 and G2 determined by MalB displacement assay: CE_{50} (cation:anion charge excess at which 50% of MalB is displaced from its complex) and EC_{50} (effective concentration at which 50% of MalB is displaced). Binding carried out in Tris-HCl buffer (10 mM, pH 7.4, 150 mM NaCl) or 100% human serum (Tris-HCl 10 mM, pH 7.4).

		Buffer	Serum
G1-L	CE_{50}	1.11 ± 0.21	1.15 ± 0.05
	EC_{50} / μM	59.9 ± 11.3	61.9 ± 2.6
G1-D	CE_{50}	0.97 ± 0.01	0.93 ± 0.16
	EC_{50} / μM	52.2 ± 0.3	50.2 ± 8.6
G2-L	CE_{50}	0.51 ± 0.05	0.85 ± 0.02
	EC_{50} / μM	13.8 ± 0.7	23.1 ± 0.5
G2-D	CE_{50}	0.63 ± 0.02	1.24 ± 0.03
	EC_{50} / μM	16.9 ± 0.5	33.5 ± 0.8

Given our surprise at the enhanced performance of spherical **G2** over worm-like **G1**, we performed ITC to validate the results. SAMul nanostructures formed by **G1-L** and **G2-L** were titrated into heparin, such that they always remained above their CMC values, to limit any effects of micelle formation on the heparin binding event. The ITC profiles for both systems had similar shapes implying similar mechanisms of complexation (Fig. 3), with each aliquot addition completely interacting with heparin. We therefore propose that complexes form without significant change in morphology. In both cases, titration endpoints were observed at a molar ratio of ca. 1.

Binding between heparin and SAMul **G1-L** and **G2-L** occurred with positive enthalpy values ΔH_{obs} of 8.03±0.17 kJmol^{-1} and 6.82±0.14 kJmol^{-1}, respectively (Fig. 3), compensated by higher positive entropy terms ΔS_{obs} (+118.8±0.6 Jmol^{-1}K^{-1} for **G1-L** and +130.2±0.6 Jmol^{-1}K^{-1} for **G2-L**, Fig. 3), which can be ascribed to the release into bulk solvent of water and counterions from the contact surfaces between the polyanion and the cationic SAMul entities. The favourable entropy is significantly greater for **G2-L** than **G1-L** – the spherical micelles based on higher generation dendritic ligands have much larger surface areas to desolvate. Endothermic, entropically-driven binding has been reported previously for electrostatic binding at charged nanoscale interfaces.[18] and we propose that it provides the driving force here. The free energy of binding ΔG_{obs} is favourable (ΔG_{obs} is -27.36±0.61 kJmol^{-1} and -31.98±0.56 kJmol^{-1} for **G1-L** and **G2-L**, respectively, Fig. 3). Most importantly, binding is stronger for **G2-L** than **G1-L** ($\Delta\Delta G_{obs}$ = 4.62 kJmol^{-1}). ITC therefore validates the MalB assay and supports the view that **G2** spherical micelles are indeed more effective heparin binders. Similar morphological effects, i.e., better binding for spherical micelles than worm-like micelles, were reported for mannopyranoside binding to Concanavalin A,[4a] and RGD peptides binding to integrins,[4c] but in those cases, the reasons were not determined. ITC suggests that, at least in

this case, better self-assembly and greater surface desolvation for spherical micelles underpin the enhanced binding effect.

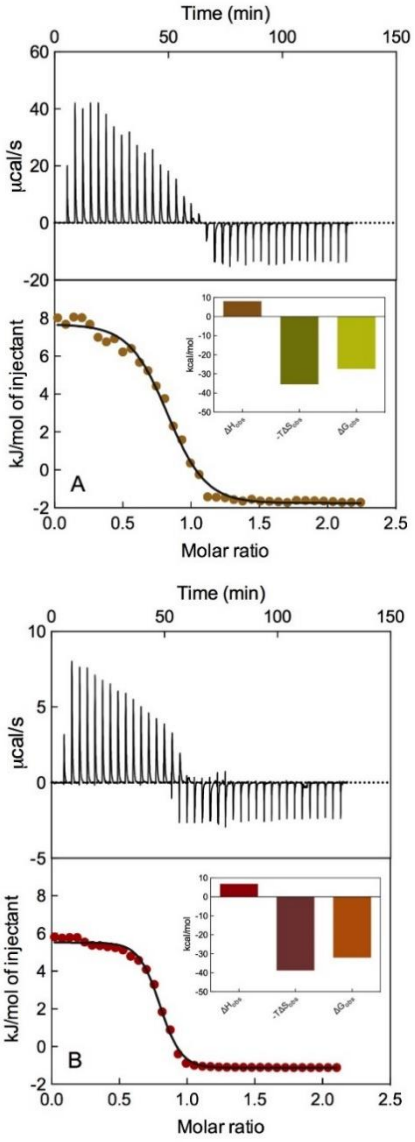

Figure 3. Titration of heparin with (A) **G1-L** and (B) **G2-L** SAMul micelles. Upper panels: raw titration data. Lower panels: ITC isotherms for **G1-L** and **G2-L** binding heparin. Inserts: thermodynamic parameters (binding enthalpy ΔH_{obs}, binding entropy $-T\Delta S_{obs}$, and binding free energy ΔG_{obs}) for **G1-L** (A) and **G2-L** (B) micelles. See ESI for details.

We were concerned that heparin binding may disrupt SAMul morphologies,[4b] and thus performed transmission electron microscopy (TEM) imaging in the absence and presence of heparin. For **G1-L** bound to heparin, we pleasingly observed the presence of worm-like micelles, which aggregated into larger hierarchical structures (see ESI). For **G2-L** bound to heparin, the spherical micelles of **G2-L** remained intact, and were also further aggregated into a hierarchical nanoscale array (see ESI). This hierarchical assembly mechanism has been discussed in detail elsewhere for electrostatically-bound micelle-polyelectrolyte complexes.[19] TEM therefore supports the morphologies predicted by modelling and suggests they are not significantly disturbed by electrostatic binding to heparin.

The relative ability of these compounds to bind heparin in much more highly competitive, and biomedically realistic conditions of 100% human serum was also monitored using our MalB assay (Table 2, Fig. 4). The spherical **G2** micelles were adversely affected by serum, with a significant rise in CE_{50} and EC_{50} values (Fig. 4, bottom), but the **G1** worm-like micelles were not (Fig. 4, top). We suggest that **G1** has greater relative lipophilicity driving self-assembly, and its nanostructures are less easily disrupted by the presence of serum albumins, which bind lipophilic groups.[20] As such, the worm-like micelles better maintain heparin binding in 100% human serum. It is known from other biomedical applications of surfactants for drug/gene delivery that spherical micelles have lower stability in challenging environments than other morphologies or stabilized micelles which can resist competition.[21] The results presented here demonstrate that morphology can also control multivalent binding strength at self-assembled nanosurfaces. The D-enantiomers were affected in the same way as their L-analogues (Table 2). Once again, differences between the enantiomers were limited – although there was some evidence that **G2-L** may be a slightly better binder than **G2-D** under these more challenging conditions, which might suggest that there is a small degree of chiral recognition at the relatively open surfaces of the spherical micelles.

Figure 4. Relative performances of compounds **G1-L** (top) and **G2-L** (bottom) in the MalB displacement assay in the absence (blue) and presence (green) of serum, demonstrated the disruption of binding experienced by compound **G2-L**.

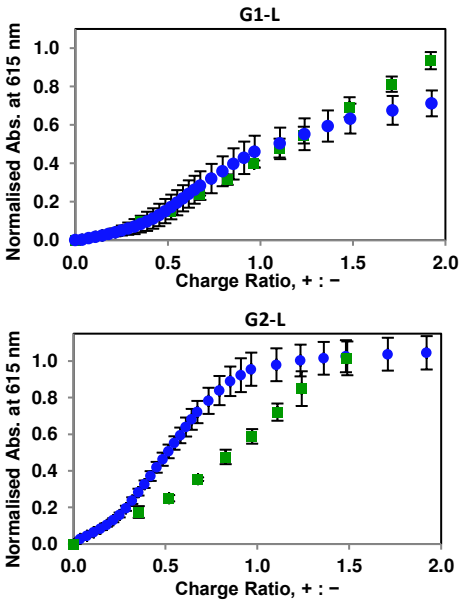

The ester linker introduces potential for these structures to degrade under physiological conditions through cleavage – switching off self-assembly and hence SAMul binding.[22] It was demonstrated by mass spectrometry that all compounds degrade under physiological pH conditions via ester hydrolysis over a 24 hour time period (see ESI), meaning these compounds have pharmaceutically useful degradation profiles for heparin reversal – any excess highly-active SAMul system will degrade to give non-self-assembling, non-active fragments.

In summary, spherical **G2** micelles are optimized for self-assembly and heparin binding in buffer as a result of the lower CMC and open dendritic surface, with accessible ligands that are desolvated on binding heparin, providing an entropic driving

force. However, worm-like **G1** micelles better retain their heparin binding in serum, while spherical micelles of **G2** are disrupted. It is clearly important to carefully consider binding environment when applying SAMul nanosystems. For *in vivo* applications, it is crucial to maximise stability and binding in challenging conditions. The ease with which molecular-scale structures can be modified and translated into programmable nanoscale morphologies is a significant advantage of the SAMul approach over other multivalent binding strategies – we suggest morphological optimization of SAMul systems will be a key strategy for a variety of biological targets

Acknowledgements

This research was funded by Marie Curie IEF 628757 for ACR and a UoY Postdoctoral Fellowship for SMB. SP wishes to acknowledge the generous financial support from the Italian Association for Cancer Research (AIRC IG 17413).

Notes and references

1 C. Fasting, C. A. Schalley, M. Weber, O. Seitz, S. Hecht, B. Koksch, J. Dernedde, C. Graf, E. W. Knapp and R. Haag, *Angew. Chem. Int. Ed.*, 2012, **51**, 10472-10498

2 (*a*) A. Barnard and D. K. Smith, *Angew. Chem. Int. Ed.*, 2012, **51**, 6572-6581. (*b*) K. Petkau-Milroy and L. Brunsveld, *Org. Biomol. Chem.* 2013, **11**, 219-232.

3 (*a*) J. E. Kingery-Wood, K. W. Williams, G. B. Sigal and G. M. Whitesides, *J. Am. Chem. Soc.,* 1992, **114**, 7303-7305. (*b*) M. R. Dreher, A. J. Simnick, K. Fischer, R. J. Smith, A. Patel, M. Schmidt and A. Chilkoti, *J. Am. Chem. Soc.,* 2008, **130**, 687-694. (*c*) M. K. Müller and L. Brunsveld, *Angew. Chem. Int. Ed.,* 2009, **48**, 2921-2924. (*d*) B. A. Rosenzweig, N. T. Ross, D. M. Tagore, J. Jayawickramarajah, I. Saraogi and A. F. Hamilton, *J. Am. Chem. Soc.,* 2009, **131**, 5020-5021. (*e*) S. K. M. Nalluri, J. Voskuhl, J. B. Bultema, E. J. Boekema and B. J. Ravoo, *Angew. Chem. Int. Ed.,* 2011, **50**, 9747-9751. (*f*) E. L. Dane, A. E. Ballok, G. A. O'Toole and M. W. Grinstaff, *Chem. Sci.,* 2014, **5**, 551-557. (*g*) M. J. Chmielewski, E. I. Buhler, J. Candau and J.-M. Lehn, *Chem. Eur. J.*, 2014, **20**, 6960-6977.

4 (*a*) B. S. Kim, D. J. Hong, J. Bae and M. Lee, *J. Am. Chem. Soc.,* 2005, **127**, 16333-16337. (*b*) J.-H. Ryu, E. Lee, Y.-b. Lim and M. Lee, *J. Am. Chem. Soc.*, 2007, **129**, 4808-4815. (*c*) D. J. Welsh, P. Posocco, S. Pricl and D. K. Smith, *Org. Biomol. Chem.*, 2013, **11**, 3177-3186. (*d*) G. Na, Y. He, Y. Kim and M. Lee, *Soft Matter*, 2016, **12**, 2846-2850. (*e*) T. Noguchi, B. Roy, D. Yoshihara, J. Sakamoto, T. Yamamoto and S. Shinkai, *Angew. Chem. Int. Ed.*, 2016, **55**, 5708-5712.

5 S. M. Bromfield, E. Wilde and D. K. Smith, *Chem. Soc. Rev.,* 2013, **42**, 9184-9185.

6 (*a*) T. Wallin and P. Linse, *J. Phys. Chem.*, 1996, **100**, 17873-17880. (*b*) C. Wang and K. C. Tam, *J. Phys. Chem. B*, 2004, **108**, 8976-8982. (*c*) D. Li and N. J. Wagner, *J. Am. Chem. Soc.*, 2013, **135**, 17547-17555. (*d*) M. Goswami, J. M. Borreguero, P. A. Pincus, B. G. Sumpter, *Macromolecules*, 2015, **48**, 9050-9059. (*e*) M. S. Sulatha, U. Natarajan, *J. Phys. Chem. B*, 2015, **119**, 12526-12539.

7 (*a*) Y.-S. Cho and K. H. Ahn, *J. Mater. Chem. B*, 2013, **1**, 1182-1189. (*b*) Y. Chen, J. Peng, M. Han, M. Omar, D. Hu, X. Ke and N. Lu, *J. Drug Targeting*, 2015, **23**, 335-346. (*c*) C. Duehrkop, G. Leneweit, C. Heyder, K. Fromell, K. Edwards, K. N. Ekdahl and B. Nilsson, *Coll. Surf. B*, 2016, **141**, 576-583.

8 (*a*) A. C. Rodrigo, A. Barnard, J. Cooper and D. K. Smith, *Angew. Chem. Int. Ed.*, 2011, **50**, 4675-4679. (*b*) S. M. Bromfield, P. Posocco, C. W. Chan, M. Calderon, S. E. Guimond, J. E. Turnbull, S. Pricl and D. K. Smith, *Chem. Sci.*, 2014, **5**, 1484-1492. (*c*) L. Fechner, B. Albanyan, V. M. P. Vieira, E. Laurini, P. Posocco, S. Pricl and D. K. Smith, *Chem. Sci.*, 2016, **7**, 4653-4659.

9 (*a*) S. M. Bromfield and D. K. Smith, *J. Am. Chem. Soc.*, 2015, **137**, 10056-10059. (*b*) C. W. Chan, E. Laurini, P. Posocco, S. Pricl and D. K. Smith, *Chem. Commun.* 2016, **52**, 10540-10543.

10 (*a*) S.-Y. Lee, G. Tae and Y. H. Kim, *J. Biomater. Sci.*, 2010, **21**, 727-739. (*b*) Y. Zhao, M. S. Lord and M. H. Stenzel, *J. Mater. Chem. B*, 2013, **1**, 1635-643. (*c*) F. Zhang, J. Fei, M. Sun and Q. Ping, *Int. J. Pharm.*, 2016, **511**, 390-402.

11 S. Valimaki, A. Khakalo, A. Ora, L.-S. Johansson, O. J. Rojas and M. A. Kostiainen, *Biomacromolecules*, 2016, **17**, 2891-2900.

12 G. L. Montalvo, Y. Zhang, T. M. Young, M. J. Costanzo, K. B. Freeman, J. Wang, D. J. Clements, E. Magavern, R. W. Kavash, R. W. Scott, D. H. Liu and W. F. DeGrado, *ACS Chem. Biol.*, 2014, **9**, 967-975.

13 K. Rajangam, H. A. Behanna, M. J. Hui, X. Han, J. F. Hulvat, J. W. Lomansey and S. I. Stupp, *Nano Lett.*, 2006, **6**, 2086-2090.

14 J. N. Israelachvili, D. J. Mitchell and B. W. Ninham, *J. Chem. Soc. Faraday Trans. 2*, 1976, **72**, 1525-1568.

15 (*a*) H.-J. Sun, S. Zhang and V. Percec, *Chem. Soc. Rev.*, 2015, **44**, 3900-3923. (b) X. Liu, J. Zhou, T. Yu, C. Chen, Q. Cheng, K. Sengupta, Y. Huang, H. Li, C. Liu, Y. Wang, P. Posocco, M. Wang, Q. Cui, S. Giorgio, M. Fermeglia, F. Qu, S. Pricl, Y. Shi, Z. Liang, P. Rocchi, J. J. Rossi and L. Peng, *Angew. Chem. Int. Ed.*, 2014, **53**, 11822-11827. (*c*) J. F. Trant, N. Jain, D. M. Mazzuca, J. T. McIntosh, B. Fan, S. M. Mansour Haeryfar, S. Lecommandeux and E. R. Gillies, *Nanoscale*, 2016, **8**, 17694-17704.

16 M. C. A. Stuart, J. C. van de Pas and J. B. F. N. Engberts, *J. Phys. Org. Chem.,* 2005, **18**, 929-934.

17 (*a*) S. M. Bromfield, A. Barnard, P. Posocco, M. Fermeglia, S. Pricl and D. K. Smith, *J. Am. Chem. Soc.*, 2013, **135**, 2911-2914. (*b*) S. M. Bromfield, P. Posocco, M. Fermeglia, S. Pricl, J. Rodríguez-López, D. K. Smith, *Chem. Commun.*, 2013, **49**, 4830-4832.

18 (*a*) C. Wang and K. C. Tam, *Langmuir* 2002, **18**, 6484-6490. (*b*) J. Courtois and J.-F. Berret, *Langmuir* 2010, **26**, 11750-11758. (*c*) M. Uchman, M. Gradzielski, B. Angelov, Z. Tošner, J. Oh, T. Chang, M. Štěpánek and K. Procházka, *Macromolecules* 2013, **46**, 2172-2181. (*d*) L. Vitorazi, N. Ould-Mouassa, S. Sekar, J. Fresnais, W. Loh, J.-P. Chapel and J.-F. Berret, *Soft Matter* 2014, **10**, 9496-9505.

19 V. M. P. Vieira, V. Liljeström, P. Posocco, E. Laurini, S. Pricl, M. A. Kostiainen and D. K. Smith, *J. Mater. Chem. B*, 2017, **5**, 341-347.

20 (*a*) U. Kragh-Hansen, *Pharm. Rev.*, 1981, **33**, 17-53. (*b*) U. Kragh-Hansen, V. T. G. Chuang and M. Otagiri, *Biol. Pharm. Bull.*, 2002, **25**, 695-704. (*c*) M. Fasano, S. Curry, E. Terreno, M. Galliano, G. Fanali, P. Narciso, S. Notari and P. Ascenzi, *IUBMB Life*, 2005, **57**, 787-796.

21 (*a*) S. Tenjarla, *Crit. Rev. Ther. Drug Carrier Syst.*, 1999, **16**, 461-521. (*b*) S. Gupta, S. P. Moulik, *J. Pharm. Sci.* 2008, **97**, 22-45. (*c*) S. Kim, Y. Shi, J. Y. Kim, K. Park and J.-X. Cheng, *Expert Opin. Drug Deliv.*, 2010, **7**, 49-56. (*d*) M. J. Lawrence and G. D. Rees, *Adv. Drug Deliv. Rev.*, 2012, **64**, 175-193.

22 A. Barnard, P. Posocco, S. Pricl, M. Calderon, R. Haag, M. E. Hwang, V. W. T. Shum, D. W. Pack and D. K. Smith, *J. Am. Chem. Soc.*, 2011, **133**, 20288-20300.

Morphological Control of Self-Assembled Multivalent (SAMul) Heparin Binding in Highly Competitive Media

Graphical abstract

Shape control – self-assembly of ligands into different morphologies directs their ability to bind heparin.